Nuclear Engineering and Design 278 (2014) 618–626

Contents lists available at ScienceDirect

Nuclear Engineering and Design

journal homepage: www.elsevier.com/locate/nucengdes

Conceptual design of pressure-tube super critical water reactor with inverted geometry

Ammar Ahmad [a,b], Liangzhi Cao [a,b,*], Hongchun Wu [b], Chuanqi Zhao [b]

[a] Key Laboratory of Thermo-Fluid Science and Engineering of MOE, School of Energy and Power Engineering, Xi'an Jiaotong University, Xi'an, Shaanxi 710049, China
[b] School of Nuclear Science and Technology, Xi'an Jiaotong University, Xi'an 710049, China

HIGHLIGHTS

- Conceptual design for pressure tube SCWR with inverted geometry.
- Coupled neutronics/thermal hydraulics analysis for inverted design.
- Two pass water flow scheme and different axial fuel enrichments.
- Fuel loading pattern and control rod pattern have also been proposed.
- Lower MCST and negative void reactivity effect.

ARTICLE INFO

Article history:
Received 22 May 2014
Received in revised form 29 July 2014
Accepted 7 August 2014

ABSTRACT

An innovative core design with inverted geometry configuration has been proposed for pressure-tube type supercritical water reactors. The relative positions of fuel and coolant have been inverted and U–Th–Zr-hydride fuel was used. Two-pass water flow scheme has been selected with the assemblies at the periphery of the core having downward flow. Fuel loading pattern and control rod loading pattern have also been proposed in order to achieve more uniform radial power distribution, high coolant outlet temperature and low cladding surface temperature. Three different axial enrichments were used for fuel to reduce the axial power peak which in turn resulted in lower cladding surface temperature. A coupled neutronics and thermal hydraulics analysis was performed for the proposed inverted pressure tube type (IPTT) SCWR and an equilibrium core was analyzed. The results show that, this concept has potential benefits in reducing the clad surface temperature and increasing the life cycle length.

1. Introduction

A nuclear power plant operating above thermodynamic critical point of water (374 °C and 22.1 MPa) is known as super critical water reactor (SCWR). Unlike PWRs and BWRs, pressurizers, steam generators, recirculation pumps, steam separators and dryers are not required in SCWRs, hence they are more simple in design and are considered as the next logical extension of existing water cooled reactors. Moreover it is more economical because of its high steam enthalpy which makes compact turbine system and higher thermal efficiency of approximately 45% (Ammar et al., 2014; Zhao et al., 2013). The pressure vessel and pressure tube are the two main types of SCWRs.

Many aspects of SCWRs have been under considerations for past few years, pre-conceptual core design is one of them. A large number of core designs for SCWRs have been proposed in past studies. Both thermal (Yamaji et al., 2005) and fast (Yoo et al., 2006) neutron spectrum cores have been under consideration for SCWR pre-conceptual designs.

In recent studies on SCWRs, the scientists and researchers have proposed and optimized several assembly (Feng et al., 2014) and core (Ammar et al., 2014) designs for pressure-tube type reactors to reduce the maximum cladding surface temperature (MCST) below the design criterion. However, in spite of much devoted efforts in the recent past to optimize the core design, the current R&D activities going on SCWR technology are still facing two main challenges. One is to reduce the MCST to fulfill the development progress of cladding material. The other is to increase the fuel utilization

* Corresponding author at: School of Nuclear Science and Technology, Xi'an Jiaotong University, Xi'an 710049, China. Tel.: +86 2982663285; fax: +86 2982668916/2982667802.
E-mail addresses: caolz@mail.xjtu.edu.cn, caoliangzhi@gmail.com (L. Cao).

http://dx.doi.org/10.1016/j.nucengdes.2014.08.016
0029-5493/

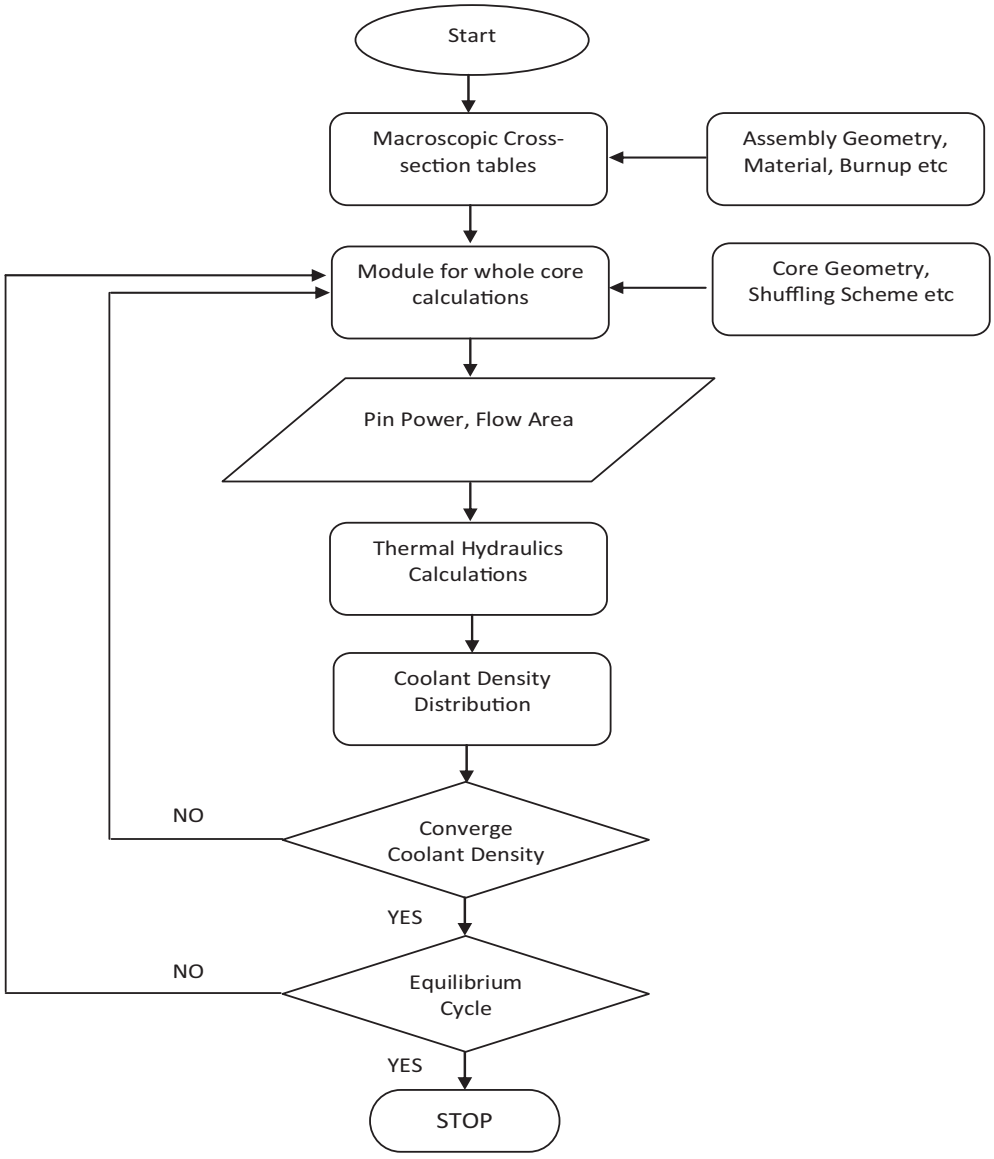

Fig. 1. Flow diagram for coupling scheme.

rate (or to reduce the initial fuel enrichment) to enhance its sustainability. Recently, an innovative concept with inverted geometry design was proposed for PWRs with several advantages (Ferroni, 2010). The inverted design consists of a block of fuel, perforated with cylindrical coolant channels, similar to the fuel concept proposed for gas cooled fast reactors (tube in duct fuel assembly). Past studies of inverted design in PWRs have proved that there are some advantages of inverted configuration such as no grid spacers are required, no flow induced vibration (FIV), reduced core pressure drop, more heavy metal loadings, allows high burnups and can give high power densities (Ferroni, 2010). Moreover inverted geometry can offer some economical benefits by optimizing the cost affecting parameters like power density (affecting capital cost), specific power (affecting fuel cycle cost) and cycle length (affecting operation and maintenance cost). For an ideal design these three factors would increase simultaneously to decrease the cost, but because of the complementary requirements of neutronics, thermal hydraulics and fuel performance, all these three parameters cannot be increased concurrently. Different inverted geometry configurations can provide economical advantages over standard pin type geometry by optimizing one or two of the above mentioned cost affecting parameters (Malen et al., 2009). So keeping in view the challenges faced by SCWR technology and the advantages offered by inverted geometry in PWRs, it is meaningful to apply this concept to SCWRs. It will not only help to overcome the existing challenges of SCWR technology but also provide some additional advantages which have been already proved for PWRs.

In this study the inverted geometry concept described above has been applied to pressure tube type SCWR and based on this concept a new design has been proposed and analyzed. U–Th–Zr-hydride fuel was selected for this design because of the negligible fission gas release which is a necessity for this type of inverted geometry and pre-hydriding of metal structure is required for effective drilling (Ferroni, 2010).

A coupled neutronics and thermal hydraulics analysis was performed for IPTT-SCWR because of the large axial variation in the coolant density throughout the fuel length. Traditional design studies which consider constant coolant density throughout the active length of fuel cannot be applied here in the case of SCWRs. So the design studies of the SCWRs need coupled calculations for both neutronics and thermal hydraulics. The research done in the past has shown that the difference between the coupled and non-coupled calculations is noticeable (Waata, 2006; Chaudri et al., 2012).

In the present study, 3D neutronics and thermal hydraulics calculations have been done on IPTT-SCWR conceptual design and based on this analysis, an assembly and core design has been proposed. Neutronics calculations were carried out by 3D fine mesh diffusion theory code while thermal hydraulics calculations were based on single channel model. External coupling technique was used to couple these two codes; it means that the required data will be exchanged between these two codes. Furthermore a core fuel loading pattern and control rod loading pattern were also searched and optimized to achieve flat radial power distribution.

2. Core design tools and models

The DRAGON code (Marleau et al., 2010) based on transport theory with a 69-group cross section library was used for two dimensional lattice calculations. The burnup dependent macroscopic group constants for assembly were generated and given as input to a 3D fine mesh diffusion theory code CITATION (Fowler and Vondy, 1971) for whole core calculations. The macroscopic group constants corresponding to all anticipated water densities in the core were generated. A supporting code was developed for core depletion calculations (Yang et al., 2011). The calculations were based on four energy groups macroscopic cross-sections obtained from assembly burnup. The radial mesh size of 1.6 cm × 1.6 cm and axial mesh size of 16.6 cm were used in the neutronics calculations. The coarse mesh in axial direction is of 50 cm and this same mesh size is used in thermal-hydraulics calculations. Quarter core symmetry was used for whole core calculations.

As there is no cross flow between coolant channels, the single channel model was used for thermal hydraulics calculations. Each assembly was represented by two typical single-channels, hot channel with maximum power and average channel with average power. The power profile for the core calculated by CITATION was given as input to the thermal hydraulics code. Flow rate for each assembly was searched using maximum power and MCST criterion. Then this flow rate distribution and average power for each assembly were used to calculate coolant density distribution. Downward flow mode was used for the peripheral assemblies and upward flow mode was used for central assemblies of the core. This coolant density distribution was then fed back as input to the neutronics code and the process was repeated until the convergence criteria for both the burn up and thermal calculations were met. Dittus–Boelter correlations were used for heat transfer coefficient calculations (Kamei et al., 2006).

A link code was used to exchange required data between these two codes. The input for one code was prepared from the output of the second code with the help of a link code. The overall flow diagram of the coupled system is shown in Fig. 1.

The equilibrium core was also searched during the procedure. The equilibrium core is defined as the core in which the burnup distribution and water density distribution at the beginning of (n)th cycle (BOC) are identical to those at the beginning of ($n+1$)th cycle. After determining all core design parameters, the first cycle is computed with neutronic/thermal hydraulics coupled system until water density distributions are converged. Then, according to fuel reload pattern, burnup distribution of the second cycle is obtained. The core calculations for one cycle of operation, followed by the shuffling of fuel assemblies, are repeated until the BOC burnup distribution is converged. Equilibrium cycle is achieved when BOC burnup distribution is converged (Zhao et al., 2013; Ammar et al., 2014). The flow diagram for assembly and core design procedure is shown in Fig. 2. As there is no phase change in SCWRs so MCST is taken as design criteria for SCWRs, fuel assembly design and core design were repeatedly changed until design criteria were met.

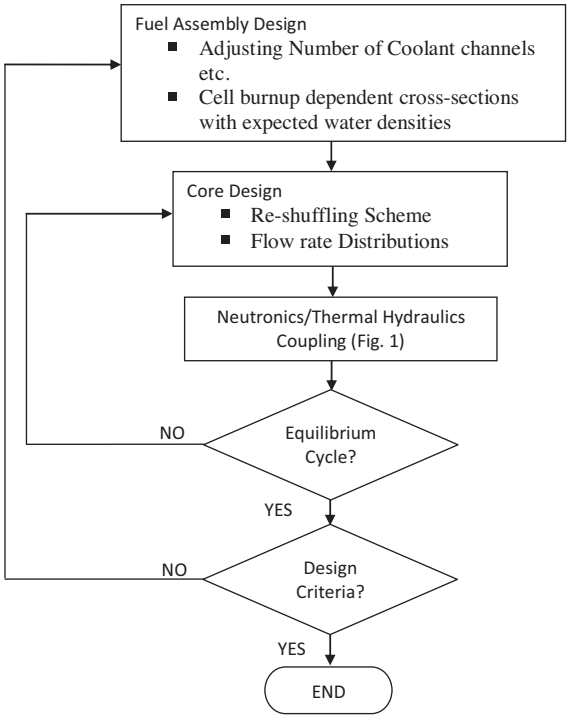

Fig. 2. Overall design procedure.

3. Fuel assembly design

Cross-sectional view of fuel assembly is shown in Fig. 3. It consists of 92 coolant channels and 10 control rod guide tubes arranged in five concentric rings, each ring has two control rod guide tubes. These 10 control rod guide tubes can allow the insertion of cluster of 10 rods made up of boron carbide (B_4C). Every coolant channel has inner diameter of 0.88 cm and clad thick is of 0.06 cm. These dimensions were selected in order to achieve better heat transfer. As heat transfer coefficient between coolant and cladding strongly depends upon coolant flow area or hydraulic diameter, so number of coolant channels and coolant channel diameter were selected to enhance heat transfer coefficient between coolant and cladding which in turn lead to lower cladding surface temperature. As this is inverted geometry so coolant channels are surrounded by fuel, the fuel thickness between coolant channels is also an important parameter in inverted configuration. The performance of inverted pressurized water reactors degrades as fuel thickness between coolant channels increases, but from the mechanical or manufacturing point of view the minimum allowable fuel thickness is 2 mm (Ferroni, 2010). So keeping in view this constraint, the coolant channels were arranged in concentric rings with the distance of 2 mm between the coolant channels of one ring to the channels in adjacent ring. The outermost component of the assembly is pressure tube made up of zirconium based alloy. Inside pressure tube there is also a solid zirconia insulator which isolates pressure tube from high temperatures. The pressure tube is in direct contact with the heavy water moderator. The materials of pressure tube, insulator, metal liner and coolant channel cladding are same as used in recent Canadian high efficiency re-entrant channel design (HERC) presented in Pencer et al. (2013) and Dominguez et al. (2013). Hydride fuel ($UTh_{0.5}Zr_{2.25}H_{5.625}$) has been used because of negligible fission gas released in this fuel (Ferroni, 2010). In analysis presented in Ferroni (2010), the uranium enrichment used was 15%, but here in this study the average enrichment used for uranium was 10%. This is due to the fact that, in this design heavy water was used for neutron moderation so initial enrichment of fuel can be decreased. Further

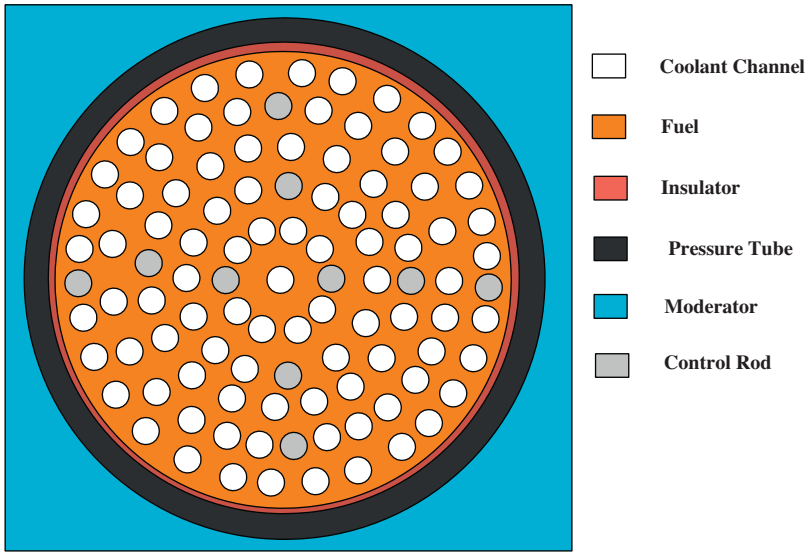

Fig. 3. Cross-sectional view of fuel assembly.

details of assembly design are shown in Table 1. The coolant void reactivity (CVR) for the assembly design is given in Fig. 4. CVR is negative and decreases with void fraction and burnup, which ensures the inherent safety feature of the design in case of loss of coolant accident (LOCA).

4. Core design

4.1. Design summary

The reactor core is a three batched refueling core operating at pressure of 25 MPa. The core generates the thermal power of 2540 MW and corresponding electrical power of 1200 MW assuming 48% efficiency. It consists of 336 fuel assemblies and average inlet and outlet temperatures are 350 °C and 625 °C respectively. The height of the core is 600 cm including 50 cm thick upper and lower axial heavy water reflector.

The principles considered to ensure the fuel and core safety are

- Negative void reactivity effect (Zhao et al., 2013)
- MCST less than 850 °C (Yang et al., 2011)
- Core shutdown margin greater than or equal to 1%dk/k (Zhao et al., 2013)

Table 1
Geometrical specifications of fuel assembly.

Component	Dimensions
Central coolant tube	0.44 cm inner radius, 0.06 cm thick
First ring of coolant tubes (8 + 2)	0.44 cm inner radius, 0.06 cm thick, 1.7 cm circle radius
2nd ring of coolant tubes (13 + 2)	0.44 cm inner radius, 0.06 cm thick, 2.9 cm circle radius
3rd ring of coolant tubes (18 + 2)	0.44 cm inner radius, 0.06 cm thick, 4.1 cm circle radius
4th ring of coolant tubes (23 + 2)	0.44 cm inner radius, 0.06 cm thick, 5.3 cm circle radius
5th ring of coolant tubes (29 + 2)	0.44 cm inner radius, 0.06 cm thick, 6.5 cm circle radius
Liner tube	7.20 cm (IR), 0.05 cm thick
Insulator	7.25 cm IR, 0.55 cm thick
Outer liner	7.80 cm IR, 0.05 cm thick
Pressure tube	7.85 cm IR, 1.2 cm thick
Fuel bundle heated length	500 cm
Assembly pitch	25 cm
Fuel material	Hydride fuel ($UTh_{0.5}Zr_{2.25}H_{5.625}$)

4.2. Fuel loading pattern

Core loading pattern has a strong impact on the performance of the core. Cladding surface temperature can be decreased by selecting the core loading pattern having more uniform radial power distributions. So the core shuffling scheme was selected in order to get flat power distribution and lower power peaking factor. The selected core loading pattern is shown in Fig. 5. Fresh fuel elements are distributed in the core and there are twice burnt fuels in the vicinity of each fresh fuel in order to achieve flat radial power distribution. Moreover, a large number of fresh fuel assemblies are loaded at the periphery of the core to avoid power peaking at the center of the core.

4.3. Axial fuel enrichment

Axial power peak has a strong effect on MCST. In order to lower down the axial power peak, different axial enrichments were used from top to bottom. When control rods were inserted from the top, the power peak at the bottom became very high i.e. more than 2.

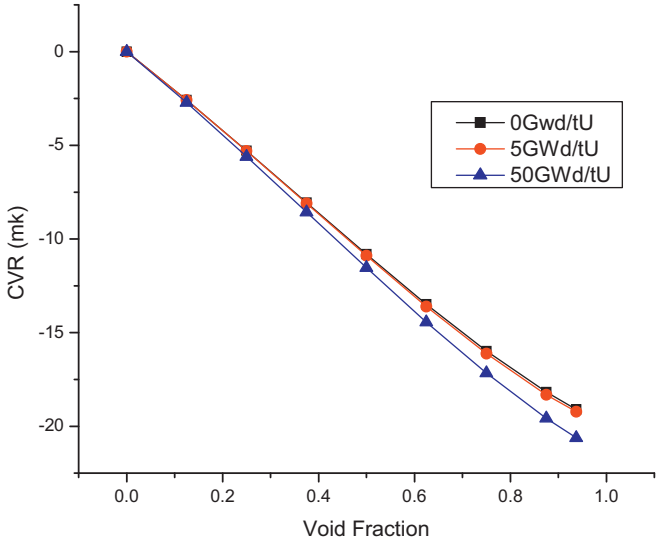

Fig. 4. Coolant void reactivity effect.

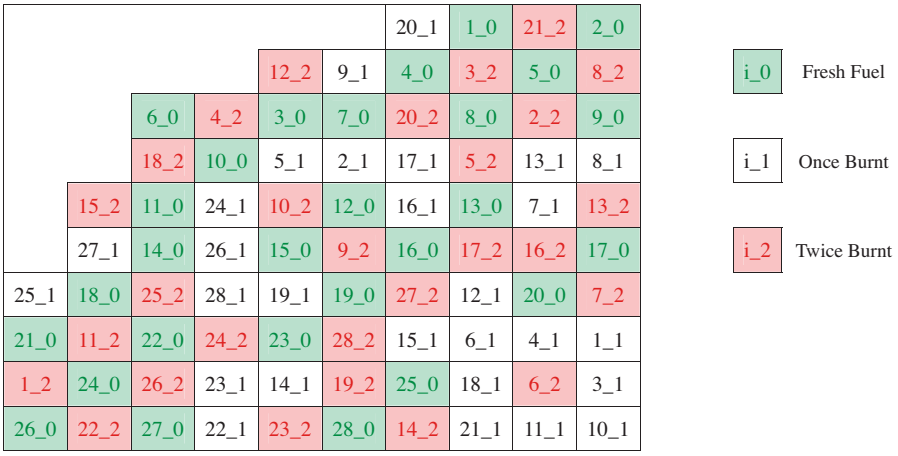

Fig. 5. Core loading pattern for quarter core.

The presence of control rods and lower coolant density at the top causes a decrease in power peak at the top and increase in power peak at the bottom of the core. In order to control this power peak, the fuel enrichment at the bottom was decreased and at the top it was increased. The fuel assembly is axially divided into three enrichments as shown in Fig. 6. The average enrichment of 10% is maintained so that cycle length of the core is not disturbed.

4.4. Control rod pattern

Control rods are mandatory for plant control; they can provide operation flexibility by controlling power throughout the burnup cycle. Fig. 7 shows radial positions of control rods inside core. The control rods are divided into seven groups on the basis of symmetry. Each group contains at most two control rods and during burnup cycle these control rods have the same withdrawn pattern. These groups are indicated form G1 to G7 in Fig. 7. Control rods are adjusted at every burnup step, to compensate fuel burnup and production of fission products etc. and to maintain average coolant outlet temperature of 625 °C and MCST under design limits. They also maintain excess reactivity, radial and axial power distributions.

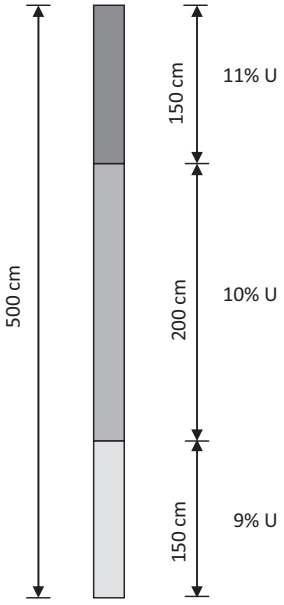

Fig. 6. Axial fuel enrichment.

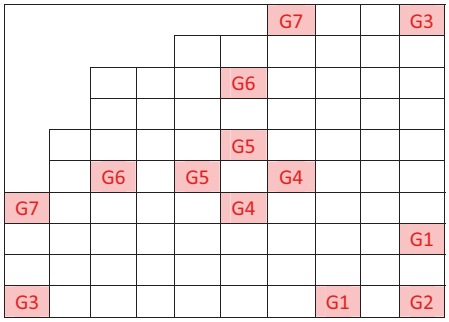

Fig. 7. Group numbers for control rods.

Fig. 8 is representing axial positions of control rods during burnup cycle. Seven columns at each burnup step are representing seven control rod groups (G1–G7). *Y*-axis represents the distance between the bottom of the control rod and bottom of the core and *X*-axis represents the burnup step number. If the distance below control rod is 500 cm, it shows that the control rod is fully withdrawn.

5. Results of equilibrium core

The primary system parameters for equilibrium core are shown in Table 2.

5.1. Coolant flow rate distribution

Two pass flow scheme was used for core, the coolant first flows downward from the peripheral assemblies and then moves upwards from the inner assemblies. White boxes in Fig. 9 show

Table 2
Preliminary core parameters.

Parameters	Results SCWR-inverted design
Thermal/electrical power (MW)	2540/1200
Average initial wt% of U^{235} (%)	10
Average exit burnup (MWd/kg)	40.86
Excess reactivity BOC/EOC (mk)	99.8/23.7
Cycle length EFPD	425
Mass flow rate (kg/s)	327
Average power density (W/cm^3)	183
Channel power peaking factor (BOC/EOC)	1.32/1.23
Axial power peaking factor	1.21/1.38
Average outlet temperature (°C)	625
MCST (BOC/EOC) (°C)	837/812

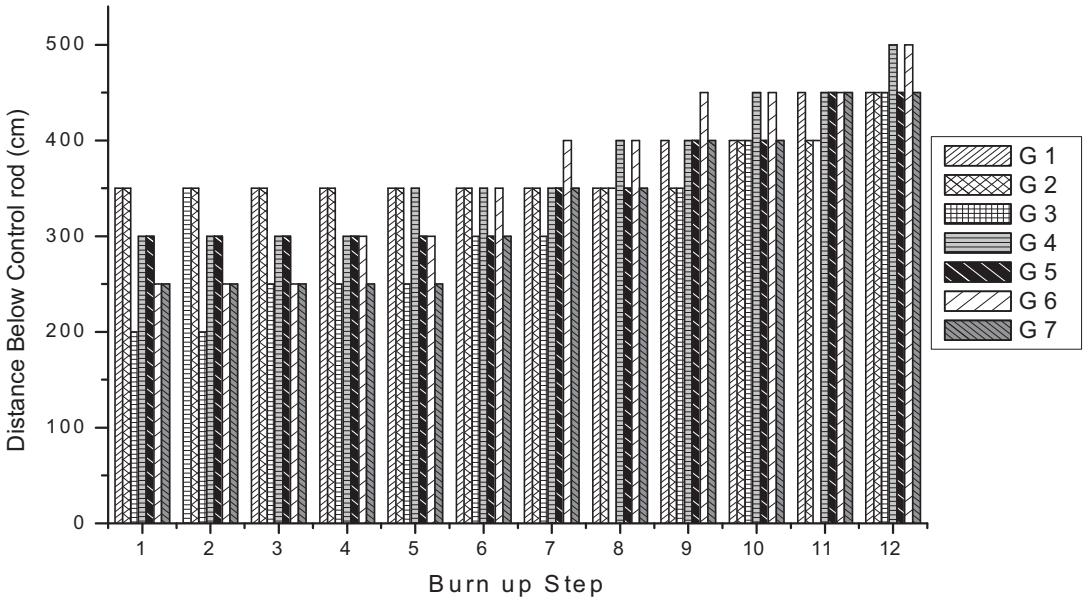

Fig. 8. Control rod pattern.

the inner assemblies having upward flow and gray boxes show the peripheral assemblies having downward flow. Upward flow rate distribution through all the inner assemblies was searched throughout the burnup cycle to satisfy the MCST criterion. Then for each inner assembly maximum flow rate among all the burnup steps was chosen. The total flow rate for peripheral assemblies was considered as equal to the total flow rate for inner assemblies. Fig. 9 shows the coolant flow rate distribution for quarter core. The numbers shown in Fig. 9 are the ratios of the flow rate of each assembly to the average flow rate for all assemblies, −1.00 in each gray box means flow rate in each peripheral assembly is same and coolant is flowing downwards through these assemblies.

5.2. Radial and axial power distribution

The axially averaged normalized radial power distribution for quarter core at beginning of cycle (BOC) and end of cycle (EOC) is shown in Fig. 10. The radial power peaking factors at BOC and EOC are 1.32 and 1.23 respectively. At EOC, the radial power distribution becomes more uniform as compared to power distribution at BOC. The axial power distribution is shown in Fig. 11. The axial power at BOC is asymmetric having peak of 1.21 at the bottom of the core, this is due to the fact that at BOC, higher water density at bottom of the core is providing better moderation and presence of the control

						-1.00	-1.00	-1.00	-1.00
				-1.00	-1.00	-1.00	-1.00	-1.00	-1.00
		-1.00	-1.00	-1.00	-1.00	1.03	1.03	1.03	1.09
		-1.00	-1.00	1.05	1.05	0.99	0.94	0.93	0.98
	-1.00	-1.00	0.99	1.08	1.13	1.10	1.10	0.96	1.10
	-1.00	-1.00	1.07	1.07	0.91	1.12	0.91	1.06	1.08
-1.00	-1.00	0.95	0.97	1.08	1.09	0.97	1.10	1.10	0.99
-1.00	-1.00	1.05	1.01	1.03	0.86	0.99	0.98	0.99	0.97
-1.00	-1.00	0.96	0.96	0.90	0.85	1.06	0.96	0.84	0.95
-1.00	-1.00	1.14	1.00	0.97	1.01	0.85	0.87	0.82	0.86

Fig. 9. Coolant flow rate distribution for quarter core.

rods in upper region. As the burnup proceeds and control rods are withdrawn power peak moves upwards and at EOC the power peak is 1.38 at about 200 cm form the bottom of the core. The small peaks appearing at 450 cm in Fig. 11 both at BOC and EOC are due to the high enrichment (11%) in this region. In the upper region the enrichment was kept high to compensate the low coolant density and presence of control rods in this upper portion of the core.

5.3. Coolant temperature and MCST distribution

The average coolant out let temperature of the core is 625 °C and outlet temperature distribution for the core is given in Fig. 12. Gray boxes at the periphery indicate the downward flow. At BOC temperature ranges from 533 °C to 713 °C. At EOC the coolant temperature distribution becomes more uniform because of more flat power distribution and it ranges from 525 °C to 690 °C. MCST distribution for quarter core is shown in Fig. 13, at BOC and EOC the MCSTs are 837 °C and 812 °C respectively. MCST throughout the burnup cycle is under design limitation i.e. less than 850 °C for pressure tube type reactors. From Table 2, it can be seen that average exit burnup for the proposed core is 40.86 MWd/kg.

5.4. Effect of heat transfer correlations on MCST

The calculations for MCST are mainly dependent on the heat transfer correlations. A sensitivity analysis has been done for MCST using following four heat transfer correlations.

- Dittus–Boelter (Dittus and Boelter, 1930)
- Oka–Koshizuka (Kitoh et al., 1999)
- Bishop (Bishop et al., 1964)
- Swenson (Swenson et al., 1965)

The MCST and average outlet temperature calculated by using these four correlations are shown in Table 3. The flow rate is kept constant for all four cases. MCSTs calculated by Dittus–Boelter, Oka and Bishop are close to each other with a maximum difference of 20 °C between Oka and Bishop. However MCST calculated by Swenson is high and has difference of 55 °C with Dittus–Boelter. Dittus–Boelter correlation has been selected for the analysis presented in this paper because the properties of coolant at high

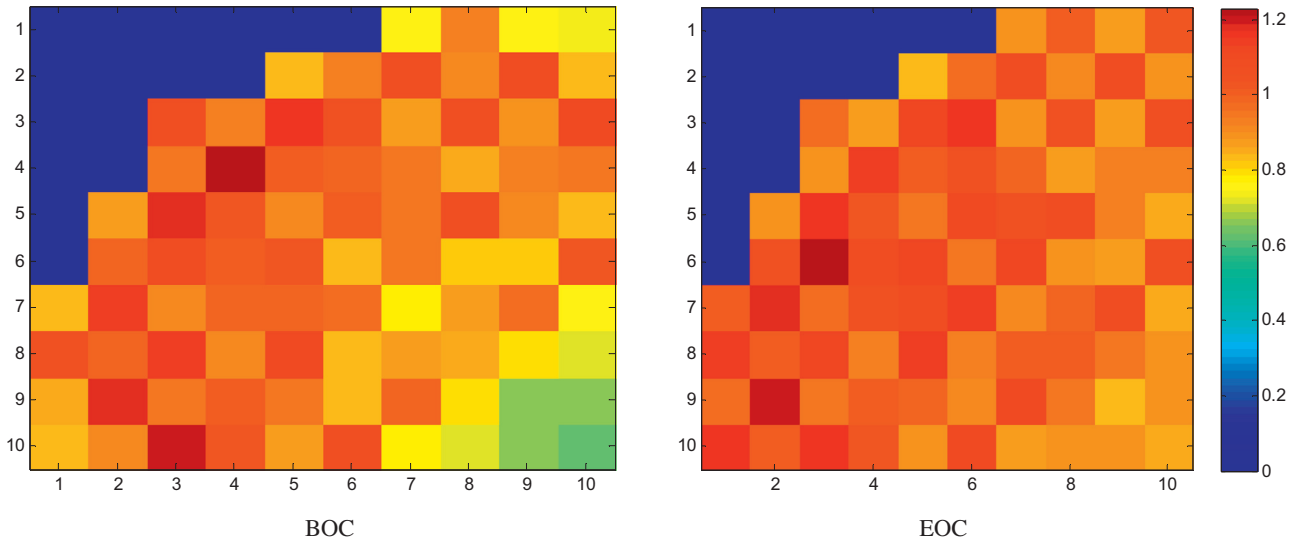

Fig. 10. Normalized radial power distribution for quarter core.

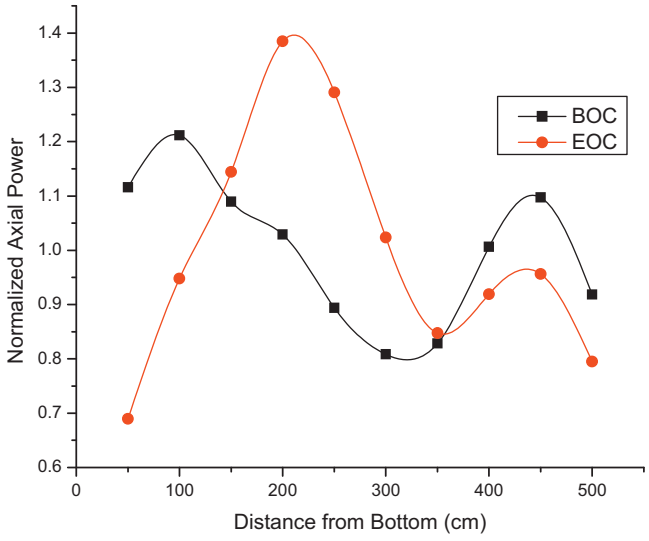

Fig. 11. Normalized axial power.

temperatures above 500 °C are same as those of gas and the well known Dittus–Boelter correlation predicts MCST better than other correlations, as it has a high accuracy for such single-phase flows (Kamei et al., 2006).

5.5. Void reactivity effect for equilibrium core

The void reactivity effect for equilibrium core was also calculated by considering total loss of coolant. The effects at BOC and EOC are −0.6%dk/k and −0.55%dk/k respectively. The design criterion of negative void reactivity effect is satisfied.

Table 3
Effect of heat transfer correlations on MCST.

Heat transfer correlation	Average outlet temperature (°C)	MCST BOC/EOC (°C)
Dittus–Boelter	625	837/812
Oka–Koshizuka	625	821/796
Bishop	625	841/819
Swenson	625	892/864

5.6. Shutdown margin

Shutdown margin was calculated at BOC of the equilibrium core. During this evaluation coolant temperature inside core was considered as same as the inlet temperature and corresponding density of 0.6 g/cc was used and it was also assumed that the control rod cluster having maximum worth was stuck at its position. In order to provide sufficient negative reactivity, 24 banks of shutdown rods were introduced in the core. The positions of control rod cluster having maximum worth and shutdown banks are shown in Fig. 14.

In Fig. 14 the gray box is indicating the position of control rod cluster having maximum worth and number inside the box is showing the axial position at which this cluster was stuck. It means that there are seven axial mesh positions below the bottom of control rod. The alphabetical digits from “A” to “X” are showing the positions of shut down banks. The effective multiplication factor for the core was calculated to be 0.984 thus having shutdown margin of −1.5%dk/k. As there are many shut down rods which are required for cold shutdown so another design of shutdown rods was also considered in this research.

Instead of inserting shutdown rods inside assembly, the “+” shaped shutdown rods were inserted in space between the assemblies as shown in Fig. 15. The same analysis of cold shutdown margin was repeated using these “+” shaped shutdown rods by same consideration that control cluster having maximum worth is stuck at its position. Gray box in Fig. 15 is representing the control rod having maximum worth and alphabets are representing the shutdown banks. Only seven banks of shutdown rods are required in this case. The effective multiplication factor of the core is calculated to be 0.982 and so having shutdown margin of −1.8%dk/k. Cladding materials for shutdown rod was not considered in the analysis; shutdown margin will further increase by the consideration of cladding material. Either of these two shapes of shutdown rods can be used for cold shutdown of the reactor.

5.7. Comparison with pin type core design

The detailed comparison between pin type and inverted geometry for PWRs has already been done in the past by Malen et al. (2009) and Ferroni (2010). The comparison of some parameters of IPTT-SCWR design and the traditional pressure tube type SCWR design presented in Ammar et al. (2014) is shown in Table 4. Although the advantages of both the geometries cannot be fully assessed from

	1	2	3	4	5	6	7	8	9	10	
A											BOC
											EOC
B											
C							589	686	603	677	
							576	628	557	603	
D					651	637	648	625	672	660	
					617	632	631	592	617	598	
E				684	588	620	606	649	645	553	
				652	586	641	609	618	610	525	
F				644	648	626	594	616	558	640	
				646	674	665	641	626	550	607	
G			650	682	629	614	571	567	610	556	
			646	674	637	666	608	586	615	573	
H			713	620	702	650	611	602	574	545	
			666	597	675	666	636	634	618	611	
I			669	694	701	663	634	585	567	533	
			628	649	670	658	642	633	647	621	
J			700	683	618	692	621	586	580	542	
			639	631	590	661	646	668	690	662	

Fig. 12. Coolant outlet temperature distribution.

	1	2	3	4	5	6	7	8	9	10	
A											BOC
											EOC
B											
C							779	801	811	810	
							729	726	708	695	
D					752	725	728	773	803	803	
					747	747	752	719	711	700	
E				795	706	684	736	742	754	745	
				780	739	727	734	729	717	726	
F				727	722	691	661	712	728	742	
				777	772	766	754	754	704	701	
G			791	782	722	688	669	686	691	670	
			812	802	795	792	740	718	713	732	
H			837	819	808	748	700	675	670	677	
			776	805	799	809	744	730	726	739	
I			831	831	826	777	722	681	651	673	
			759	759	796	765	747	744	761	744	
J			837	831	822	807	739	674	640	657	
			741	747	777	768	760	763	774	764	

Fig. 13. MCST distribution.

								N	
			H		R	F	X		
		P			V	U	A	I	
	P	B	K	Y	C	L	T	S	
H		K			Q		J	E	
		Y				D			
	R	V	C	Q			W	O	M
	F	U	L		D	W		G	7
N	X	A	T	J		O	G		
		I	S	E		M			

Fig. 14. Shutdown rods positions.

Table 4 because of the different fuel materials but some advantage of inverted design can be observed like, with low initial fuel enrichment of inverted design it is providing same cycle length of 425 days.

Cycle length can be further increased by slightly increasing the initial fuel enrichment which will in turn decrease the operation and maintenance cost of the plant. Another advantage of inverted design is to maintain same average coolant outlet temperature of 625 °C with lower MCST both at BOC and EOC. However some more research in this area is required to fully ascertain the advantages of one geometry over the other in case of SCWRs. This research should include the consideration of same fuel materials in two types of geometries, assessment of manufacturing costs of inverted geometry and irradiation tests on fuel (U–Th–Zr-hydride).

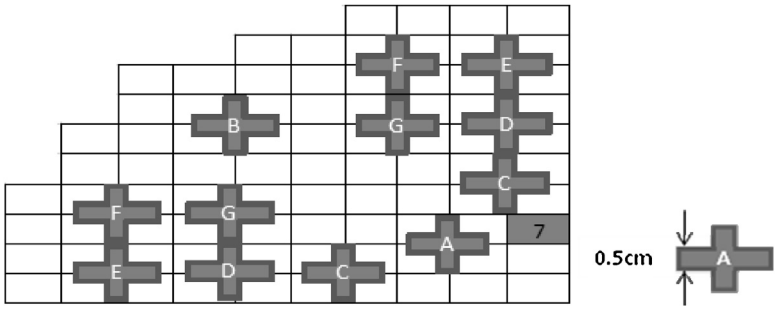

Fig. 15. Shutdown rods design and positions.

Table 4
Comparison between inverted and pin type design.

Parameters	Inverted design	Pin type design (Ammar et al., 2014)
Thermal/electrical power (MW)	2540/1200	2540/1200
Fuel	U–Th–Zr-hydride	ThO_2/PuO_2
Fuel enrichment (%)	10	13
Fuel density (g/cm^3)	9.096	9.88
Heavy metal mass in core (kg)	7.92E+04	5.69E+04
Cycle length EFPD	425	425
Average outlet temperature (°C)	625	625
MCST (BOC/EOC) (°C)	837/812	844/854

6. Conclusion

A new assembly and core design has been proposed for pressure tube type SCWRs. The proposed IPTT-SCWR design has the inverted geometry which means that the relative positions of fuel and coolant have been inverted. The core was designed and analyzed using a coupled neutronics and thermal hydraulics system. Two pass flow scheme was used for the core. Moreover control rod design and loading pattern have also been proposed. The core average coolant temperature was found to be 625 °C and MCST was found to be 837 °C. Average discharge burnup for the core is 40.86 MWd/kg and CVR is negative for the proposed assembly and core design. The results show that the design is viable from view point of neutronics and thermal hydraulics and it satisfies all the design criteria. Moreover lower MCST and longer cycle length can be achieved comparing with the traditional PT-SCWR design. However there is no experimental data available about the fuel (U–Th–Zr-hydride) performance at the elevated temperatures of SCWRs. So this is an area of research and some experimental research in this regard is also required. Furthermore the possibility of utilization of other fuels in inverted configuration also needs to be investigated in future.

Acknowledgement

This work was financially supported by the National Science Foundation of China (approved number 91126005 and 91226106).

References

Ammar, A., Cao, L., Wu, H., 2014. Coupled analysis and improvements for Canadian-SCWR core design. Nucl. Eng. Des. 268, 104–112.
Bishop, A.A., Sandberg, R.O., Tong, L.S., 1964. Forced Convection Heat Transfer to Water at Near-critical Temperatures and Supercritical Pressures, WCAP-2056, Part IV, November. Westinghouse Electric Corp., PA, USA.
Chaudri, K.S., Su, Y., Chen, R., et al., 2012. Development of subchannel code SACoS and its application in coupled neutronics/thermal hydraulics system for SCWR. Ann. Nucl. Energy 45, 37–45.
Dittus, F.W., Boelter, L.M.K., 1930. Heat Transfer in Automobile Radiators of the Tubular Type, vol. 2. Univ. of California Publ., English, Berkeley, pp. 443–461.
Dominguez, A.N., Onder, E.N., Pencer, J., et al., 2013. Canadian SCWR bundle optimization for the new fuel channel design. In: The 6th International Symposium on Supercritical Water-cooled Reactors, ISSCWR-6, Shenzhen, Guangdong, China.
Feng, J., Zhang, B., Shan, J., et al., 2014. Optimization of 54-element pressure tube SCWR bundle through neutronics/thermalhydraulics coupling analysis. Progr. Nucl. Energy 73, 1–10.
Ferroni, P., (PhD thesis) 2010. An Inverted Hydride-fueled Pressurized Water Reactor Concept. Department of Nuclear Science and Engineering, Massachusetts Institute of Technology, MA, USA.
Fowler, T.B., Vondy, D.R., 1971. Nuclear Reactor Core Analysis Code: CITATION ORNLTM-2496. Oak Ridge National Laboratory, Oak Ridge, USA.
Kamei, K., Yamaji, A., Ishiwatari, Y., et al., 2006. Fuel and core design of super light water reactor with low leakage fuel loading pattern. J. Nucl. Sci. Technol. 43 (2), 129–139.
Kitoh, K., Koshizuka, S., Oka, Y., 1999. Refinement of transient criteria and safety analysis of a high temperature reactor cooled by supercritical water. In: Proc. ICONE-7, ICONE-7234, ASME.
Malen, J.A., Todreas, N.E., Hejzlar, P., et al., 2009. Thermal hydraulic design of a hydride-fueled inverted PWR core. Nucl. Eng. Des. 239, 1471–1480.
Marleau, G., Hébert, A., Roy, R., 2010. A User's Guide for DRAGON Version 4. Institut de génie nucléaire, Département de génie mécanique, École Polytechnique de Montsréal, Montreal, Canada.
Pencer, J., Watts, D., Colton, A., et al., 2013. Core neutronics for the Canadian SCWR conceptual design. In: The 6th International Symposium on Supercritical Water-cooled Reactors, ISSCWR-6, Shenzhen, Guangdong, China.
Swenson, H.S., Caever, C.R., et al., 1965. Heat transfer to supercritical water in smooth-bore tube. J. Heat Transf. 87 (4), 477–484.
Waata, C., 2006. Coupled Neutronics/Thermal-hydraulics Analysis of a High Performance Light-water Reactor Fuel Assembly. Institute of Nuclear Technology and Energy System, University of Stuttgart, Stuttgart, Germany.
Yamaji, A., Kaemi, K., Oka, Y., et al., 2005. Improved core design of high temperature supercritical-pressure light water reactor. Ann. Nucl. Energy 32 (7), 651–670.
Yang, P., Cao, L., Wu, H., et al., 2011. Core design study on CANDU-SCWR with 3D neutronics/thermal hydraulics coupling. Nucl. Eng. Des. 241, 4714–4719.
Yoo, J., Ishiwatari, Y., Oka, Y., et al., 2006. Conceptual design of compact supercritical water-cooled fast reactor with thermal hydraulic coupling. Ann. Nucl. Energy 33, 945–956.
Zhao, C., Cao, L., Wu, H., et al., 2013. Conceptual design of a supercritical water reactor with double-row-rod assembly. Progr. Nucl. Energy 63, 86–95.